Dynamical Coulomb Blockade of Shot Noise

Carles Altimiras,* Olivier Parlavecchio, Philippe Joyez, Denis Vion, Patrice Roche, Daniel Esteve, and Fabien Portier†
Service de Physique de l'Etat Condensé (CNRS URA 2464), IRAMIS, CEA-Saclay, 91191 Gif-sur-Yvette, France
(Received 20 September 2013; revised manuscript received 6 February 2014; published 13 June 2014)

We observe the suppression of the finite frequency shot noise produced by a voltage biased tunnel junction due to its interaction with a single electromagnetic mode of high impedance. The tunnel junction is embedded in a $\lambda/4$ resonator containing a dense SQUID array providing it with a characteristic impedance in the kΩ range and a resonant frequency tunable in the 4–6 GHz range. Such high impedance gives rise to a sizable Coulomb blockade on the tunnel junction (∼30% reduction in the differential conductance) and allows an efficient measurement of the spectral density of the current fluctuations at the resonator frequency. The observed blockade of shot noise is found in agreement with an extension of the dynamical Coulomb blockade theory.

DOI: 10.1103/PhysRevLett.112.236803 PACS numbers: 73.23.−b, 72.70.+m, 73.23.Hk, 85.25.Cp

Contrary to usual electronic components for which one can define an intrinsic behavior (e.g., the I-V characteristic), the transport properties of a coherent quantum conductor depend on its biasing circuit. This is true even when the size of the circuit exceeds the electron coherence length, suppressing electronic interference effects. This nonintrinsic behavior can be traced to the quantum-probabilistic character of the transmission of electrons through the conductor, resulting in broadband fluctuations of the current called shot noise [1]. This current noise can create collective excitations (hereafter called "photons") in the electromagnetic environment seen by the conductor. This yields a backaction on the transport properties of the conductor itself [2]. This physics bears similarities with the spontaneous emission of photons by an excited atom, albeit with important differences: first, dc biased quantum conductors are out-of-equilibrium open systems and cannot be described as a set of discrete levels; second, the dimensionless parameter characterizing the electron-photon coupling is given by the ratio of the environment's impedance to the resistance quantum $R_K = h/e^2 \simeq 25.8$ kΩ; hence, by increasing the impedance of the circuit connected to the quantum conductor, one can significantly increase the effective coupling constant. This results in a rich physics, already partially understood: noticeably, the dynamical Coulomb blockade (DCB) theory [2] accounts for the observed suppression [3–5] of the low voltage conductance of a tunnel element as a result of its coupling to a dissipative electromagnetic environment. A natural step is then to understand how the coupling to the environment modifies the current fluctuations themselves: is there a Coulomb blockade of shot noise? This question of current fluctuations in the presence of DCB was addressed theoretically for the low frequency, long time limit where the corrections to the noise power and to the full counting statistics were predicted [6–9]. Instead, we consider here the environmental feedback on the frequency dependence of the shot noise of a simple quantum conductor, a tunnel junction. Following Ref. [10], we extend the DCB theory to predict the finite frequency emission noise spectrum of a voltage biased tunnel junction in the presence of an arbitrary linear environment. Probing this prediction requires achieving strong coupling of the junction to its environment and measuring its high frequency shot noise. To do so, we fabricate a tunnel junction embedded in the simplest environment, a harmonic oscillator, and measure the effect of Coulomb blockade on the shot noise power at the frequency of the oscillator. The oscillator is realized with a microwave resonator based on a Josephson transmission line allowing both a tenfold increase of the coupling constant between the junction and the resonator, and tuning the resonant frequency. The data are found in quantitative agreement with the theory.

In order to evaluate the current and its fluctuations through a tunnel element in the presence of DCB, we consider a circuit consisting of a tunnel junction of conductance G_T in series with an impedance $Z(\nu)$ described as the series combination of harmonic modes (see upper panel of Fig. 1) at temperature T and biased at voltage V. We then compute (see the Supplemental Material [11] for more details) the current I and the quantum spectral density $S_I(\nu)$ of current noise, i.e., the Fourier transform of the nonsymmetrized current-current correlator

$$S_I(\nu) = 2\int_{-\infty}^{\infty} \langle I(t)I(0)\rangle e^{-i2\pi\nu t} dt. \tag{1}$$

In this convention positive (negative) frequencies correspond to energy being emitted (absorbed) by the quasiparticles to (from) the electromagnetic modes. Taking separate thermal equilibrium averages over the unperturbed quasiparticle and environmental degrees of freedom yields

$$I(V) = \frac{G_T}{e}[\gamma \circ P(eV) - \gamma \circ P(-eV)], \tag{2}$$

 © 2014 American Physical Society

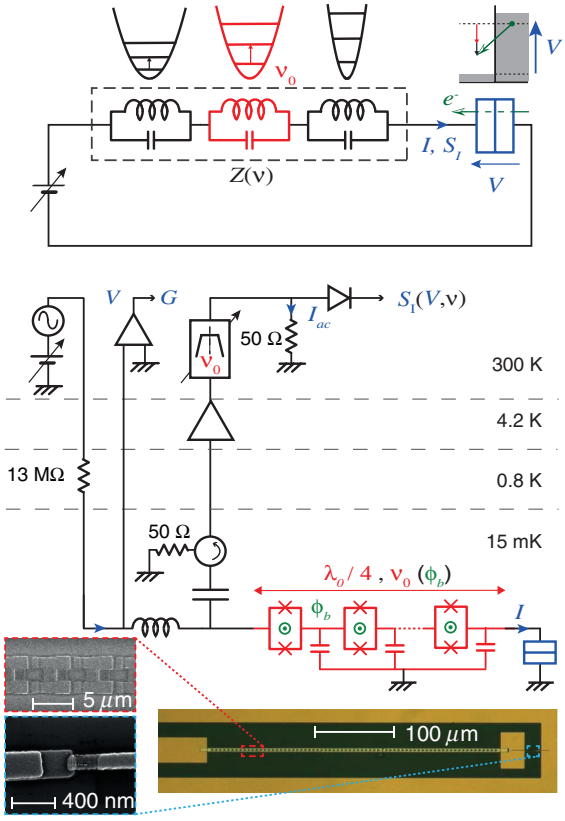

FIG. 1 (color). Coulomb blockade in a normal quantum conductor. (a) A quantum conductor (here a tunnel junction) is voltage biased (V) through a series impedance Z modeled as a collection of harmonic modes, resulting in inelastic electron tunneling. (b) Experimental setup: a tunnel junction is dc biased at voltage V, and connected to a SQUID-based resonator presenting a discrete mode at frequency ν_0, tuned by varying the magnetic flux ϕ_b threading each SQUID loop. The dc biasing line and 50Ω microwave measurement line are separated by a bias tee, allowing us to measure the junction dc differential conductance $G(V)$ and the emission noise $S_I(\nu_0, V)$. The measurement line includes an isolator, a cryogenic amplifier with 42 dB gain, a 180 MHz passband filter centered on ν_0, and a matched quadratic detector. Temperatures of the different stages are indicated on the right. Bottom illustrations: global view of the sample, with SEM pictures of SQUIDs (top inset) forming the array and of the normal tunnel junction (bottom inset), both from sample 1.

$$S_I(\nu, V) = 2G_T[\gamma \circ P(eV - h\nu) + \gamma \circ P(-h\nu - eV)], \quad (3)$$

where $\gamma \circ P(E) = \int d\varepsilon' \gamma(\varepsilon') P(E - \varepsilon')$ with $P(\varepsilon)$ the probability density for a tunneling electron to emit the energy ε in form of photons into the impedance [2], with $\gamma(\varepsilon) = \int d\varepsilon' f(\varepsilon')[1 - f(\varepsilon' + \varepsilon)] = \varepsilon/(1 - e^{-\varepsilon/k_B T})$, and with f the Fermi function. Equation (2) is the standard DCB expression for the tunneling current [2], whereas Eq. (3) is our prediction for the Coulomb blockade of shot noise, which we probe in the experiment described below. For a positive bias voltage and low temperature ($k_B T \ll eV, h\nu$), Eqs. (2) and (3) take the simpler form

$$I(V) = \frac{G_T}{e} \int_0^{eV} (eV - \varepsilon) P(\varepsilon) d\varepsilon, \quad (4)$$

$$S_I(\nu, V) = 2G_T \Theta(\mathrm{eV} - h\nu) \int_0^{eV - h\nu} (eV - h\nu - \varepsilon) P(\varepsilon) d\varepsilon, \quad (5)$$

with $\Theta(\varepsilon)$ the Heaviside function. Equations (4) and (5) are easily interpreted: the total current is proportional to the average energy available for quasiparticles upon the transfer of an electron through the circuit, and so is the noise power at frequency ν, albeit imposing the emission of a photon of energy $h\nu$ into the environment. In the case of a vanishing impedance $Z(\nu) \ll R_K$, $P(\varepsilon) = \delta(\varepsilon)$ and one recovers the standard, noninteracting, finite frequency shot noise result [12]. In the case of a discrete harmonic oscillator of frequency $\nu_0 = 1/[2\pi\sqrt{LC}]$ and impedance $Z_C = \sqrt{L/C}$, thermalized at a temperature $T \ll h\nu_0/k_B$: $P(E) = \sum_{k=0}^{\infty} p_k \delta(E - kh\nu_0)$, with $p_k = e^{-\alpha}\alpha^k/k!$ the probability for the oscillator to absorb k photons [2], and $\alpha = \pi Z_C/R_K$ the coupling strength between the tunnel junction and the oscillator. Our experiment achieves an unprecedented electron-single mode coupling $\alpha \sim 0.3$, which allows observing multiphoton processes both in the average current and in the emission noise. Note that, despite similar denominations, the effect we consider here differs from *static* Coulomb blockade, which results from the charging energy of a small island connected to reservoirs by tunnel barrier. Static Coulomb blockade is a quasiclassical effect which can be described by master rate equations, at the level of the current noise [13], and even the full counting statistics [14].

Our experimental setup is schematized in the lower panel of Fig. 1: a 100×100 nm^2 tunnel junction with tunnel resistance G_T^{-1} in the 100 kΩ range is embedded in an on-chip $\lambda/4$ coplanar resonator of resonant frequency ν_0, whose inner conductor is made of an array of identical and equally spaced Al/AlOx/Al SQUIDs. To a very good approximation, its lineic inductance is dominated by the Josephson inductance $L_J = \hbar[2eI_0|\cos(e\phi/\hbar)|a]^{-1}$, where I_0 is the maximum critical current of one SQUID, ϕ the flux applied to each SQUID, and a the distance between adjacent SQUIDs. This increases the resonator impedance Z_C above 1 kΩ, and allows us to decrease ν_0 while increasing Z_C by applying a flux through the SQUIDs. Two samples were fabricated and measured. In both cases the 6 GHz maximum frequency of the resonator ensures $k_B T \ll h\nu_0$ at the 15 mK temperature of the experiment, so that thermal fluctuations do not blur the Coulomb blockade effects. The minimum zero flux lineic inductances of the first and second resonators were designed at 8.80×10^{-5} Hm^{-1} and 3.95×10^{-4} Hm^{-1}, respectively. Note that Josephson transmission lines have been used to create nonlinear resonators used as parametric amplifiers [15], or to probe how quantum phase slips drive them into an insulating state at $Z_C \gg R_K$ [16]. We avoid this regime by keeping Z_C in

the kΩ range, which still allows us to obtain sizable DCB corrections. Keeping the current going through the resonator much smaller than I_0 ensures that the Josephson junctions can be considered as linear inductances. The resistance G_T^{-1} being much higher than $Z(\nu)$, the impedance seen by one conduction channel of the junction is not shunted by the parallel conductance of the other channels [17]. The SQUIDs and the tunnel junction were fabricated on a Si/SiO_2 substrate using standard nanofabrication techniques [11]. In addition, a $30 \times 50 \times 0.3\ \mu m^3$ gold patch is inserted between the tunnel junction and the SQUID array in order to evacuate the Joule power dissipated at the tunnel junction via electron-phonon coupling. As an example, assuming a typical 2 nW $\mu m^{-3}\,K^{-5}$ electron-phonon coupling constant [18], a 100 μV (1 mV) bias on a 200 kΩ tunnel resistance increases the electron temperature from 15 to 20 mK (50 mK), keeping heating effects negligible. Note that the thermalization pad adds an additional 12 fF to ground, which is taken into account to evaluate the total impedance seen by the tunnel junction. The chip is connected to the biasing and measurement circuits through a commercial 50 Ω matched bias tee. The inductive (low frequency) path is used both to bias the sample through a cold 13 MΩ resistor, and to measure the dc voltage across the tunnel junction and its conductance $G(V)$. The capacitive (rf) path guides the radiation $S_I(\nu, V)$ emitted by the sample to a cryogenic isolator anchored at 15 mK, to a cryogenic amplifier with a ∼2.5 K noise temperature in the 4–8 GHz bandwidth, to room temperature bandpass filters, and finally to a power "square law" detector, the output voltage of which is proportional to its input microwave power. The isolator diverts the current noise of the amplifier to a 50 Ω matched resistor that reemits to the sample a blackbody radiation only at the coldest temperature, ensuring a negligible photon occupation of the resonator at GHz frequencies. Finally, the signal $S_I(\nu, V)$ is extracted from the large noise floor of the cryogenic amplifier by a lock-in detection involving a 1 μV sinusoidal modulation at 17 Hz on top of the dc voltage V.

We first characterized the on-chip microwave resonator by measuring the power emitted by the electronic shot noise of the junction $S_I \sim 2eI$ at high bias voltage $V \sim 1$ mV [19], where DCB effects are negligible. Under these conditions, the spectral density of the emitted power is $2eV\mathrm{Re}[Z(\nu)]G_T/|1 + G_T Z(\nu)|^2 \simeq 2eVG_T\mathrm{Re}[Z(\nu)]$ since the tunnel resistance ($G_T^{-1} = 230$ kΩ/450 kΩ for sample 1/2) is much larger than the maximum detection impedance $Z(\nu)$. This spectral density is obtained using a heterodyne measurement implementing a 10 MHz-wide bandpass filter at tunable frequency. As shown in Fig. 2, the extracted $\mathrm{Re}[Z(\nu)]$ is in satisfactory agreement with predictions. In particular, $Z(\nu)$ shows the expected resonance, with a resonant frequency ν_0 decreasing with ϕ, associated to an increasing impedance and quality factor, which is limited by radiative losses. The maximum disagreement

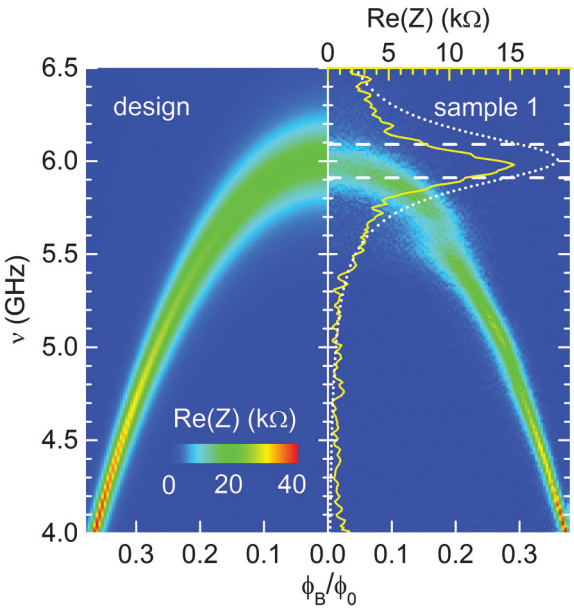

FIG. 2 (color). Characterization of the environment impedance: Designed (left) and measured (right) real part of the impedance $Z(\nu)$ of the quarter-wave resonator of sample 1 (see Fig. 1) as a function of magnetic flux ϕ_b and frequency ν. The overprinted curve on the right (top scale) shows the resonance at $\nu_0 \backsimeq 6$ GHz for $\phi_b = 0$, measured (solid line) and calculated (dotted line). Horizontal dotted white lines indicate −3 dB bandwidth used for measuring the shot noise power shown in Fig 3(a).

between the measured maximum for $\mathrm{Re}[Z(\nu)]$ and the calculated one is about 15%, which we attribute to an uncertainty in the calibration of the gain of the amplifying chain [11]. We attribute the additional structure around 5.7 GHz to a parasitic resonance in the detection chain. Once our microwave environment calibrated, we measure both the differential conductance $G(V)$ of the tunnel junction and the voltage derivative $\partial S_I(\nu_0, V)/\partial V$ of the noise emitted in a 180 MHz bandwidth centered around the resonator frequency ν_0, as a function of the dc bias voltage applied to the junction. The conductance, shown in the upper panel of Fig. 3 for both samples, is nonlinear, showing a staircase behavior characteristic of DCB corrections due to a single mode, rounded by the finite temperature [2]. The high characteristic impedance of our resonators yields DCB corrections to the conductance 10 times higher than with standard microwave resonators [19,20], and shows not only the single photon emission onset at bias voltage $V_0 = h\nu_0/e$ but also the two photon onset at $2V_0$. As shown in the lower panels of Fig. 3, the voltage derivative of emission noise power also displays a non-linear staircase shape, with a first singularity at V_0, followed by a smaller step at $2V_0$. The first step at V_0 is predicted in the standard—not including DCB effects—finite frequency shot noise theory, represented by the dotted black curve in the lower panel of Fig. 3. It has been observed in several experiments [21–24] and can be dually

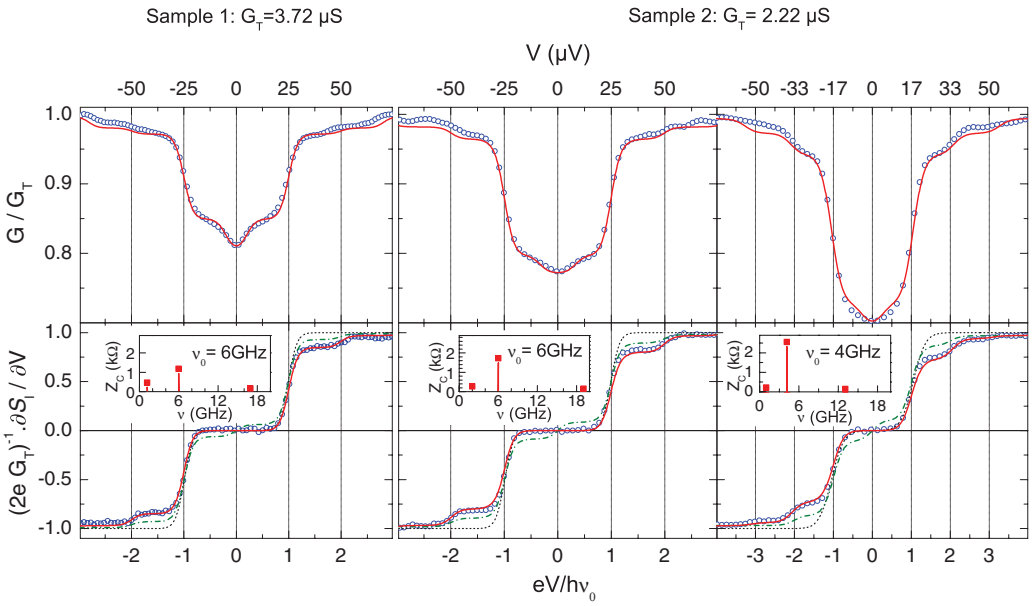

FIG. 3 (color). Comparison between the measured conductance and noise blockade, and an extension of the dynamical Coulomb blockade theory. Normalized differential conductance $G(V)$ (top) and current noise spectral density $\partial S_I(\nu_0, V)/\partial V$ (bottom). Open circles are experimental data measured at 15 mK. The left panel shows data measured on sample 1, with $\nu_0 = 6$ GHz, the center and right panel data measured on sample 2 with $\nu_0 = 6$ and 4 GHz, respectively. Solid red lines result from an analytical fit to the data involving series impedance made of three discrete modes shown in insets and the dotted black curve shows the noninteracting, finite frequency shot noise prediction. The green dot-dashed line represents the DCB expression for the current noise density symmetrized with respect to frequency.

understood either in terms of the finite time coherence of a dc biased quantum conductor, or in terms of the energy cost of creating excitations at frequency ν_0 in the measuring apparatus [12,25,26]. The second step occurs at the onset voltage for the emission of two photons in the resonator by a tunneling electron. The significant difference between the experimental points and the noninteracting prediction demonstrates the Coulomb blockade of shot noise.

We now probe how the data shown in Fig. 3 can be quantitatively accounted for by Eqs. (2) and (3), using our well-controlled environment as an input to evaluate $P(E)$. We model this environment as a series combination of three discrete harmonic modes. The two higher frequency ones correspond to the fundamental and first harmonic modes of the resonator. These two modes account with no adjustable parameters for the observed variations above $V_0 = h\nu_0/e$. Their characteristic impedance can be evaluated through the standard formula $Z_C = (2/\nu_0 \mathrm{Im}Y'(\nu_0))$, where $Y(\nu)$ is the environment's admittance, evaluated from our modeling of the Josephson transmission line. We introduce an additional lower frequency mode to account for the unexpected 3% dip in the differential conductance that we observe at low bias voltage $|V| \lesssim 5\ \mu V$. We attribute this low-frequency parasitic resonance, which only slightly affects the data, to the bias tee. The corresponding predictions, assuming an electron temperature $T_e = 16$ mK corresponding to the temperature of the refrigerator's mixing chamber, are represented by the solid red curve in the top graphs of Fig. 3. Note that at this temperature, the $\sim 3.5 k_B T/h \sim 1$ GHz smearing expected from the Fermi distribution is broader than the linewidth of the modes of our resonator. This is why the discrete modes model, which yields analytical expression for the $P(E)$ function [2], is able to reproduce the data. The emission noise data can be reproduced by Eq. (2) with excellent accuracy, whereas the expression corresponding to the current noise spectral density symmetrized with respect to frequency [10,11], $S_I^{\mathrm{sym}}(\nu, V) = [S_I(-\nu, V) + S_I(\nu, V)]/2$, represented by the green dash-dotted line in Fig. 3, is not compatible with our data. Note that at low temperature $k_B T \ll h\nu_0$ the relative size of the two-photon step is $\alpha/2$, which explains why noise blockade is not seen with usual environment impedance yielding values of $\alpha \sim 10^{-3}$. However, when considering the proposed primary shot noise thermometry [27], even such low values of α cause a systematic correction that should be considered to reach metrological accuracy. Last, the data shown in the to left panels of Fig. 3 were taken for the maximum value of $\nu_0 = 6$ GHz. Applying a flux through the SQUIDs induces a stronger blockade due to the increased Josephson inductance. As shown on the right panel of Fig. 3, the higher impedance of sample 2 allows observing even three-photon processes when the resonant frequency is set at 4 GHz (the lower end of our detection bandwidth), yielding $Z_C \simeq 2.25$ kΩ and a 30% reduction of the zero-bias conductance.

In conclusion, we have developed an original electromagnetic environment, allowing us to reach an

unprecedented coupling between a quantum conductor and a single mode environment. We took advantage of this to demonstrate the Coulomb blockade of the finite frequency noise of a tunnel junction. Two- and three-photon processes are identified, in agreement with an extension to the theory of dynamical Coulomb blockade. The experimental methods developed here can be readily applied to quantum conductors of arbitrary transmissions, for which a complete description of quantum transport in the presence of an electromagnetic environment is still missing. Noticeably, they allow us to probe the Coulomb blockade of shot noise in quantum point contacts [28–33], where DCB was recently demonstrated to bear a deep connection to the physics of impurities in Luttinger liquids [34], or quantum dots, where the interplay between resonant tunneling through the dot and the coupling to the environment was mapped to the physics of Majorana fermions [35].

This project was funded by the CNano-IDF Shot-E-Phot and Masquel, the Triangle de la Physique DyCoBloS and ANR AnPhoTeQ grants. Technical assistance from Patrice Jacques, Pierre-François Orfila, and Pascal Sénat, as well as discussions within the Quantronics group, with Inès Safi, Pascal Simon, and Jean-René Souquet are gratefully acknowledged.

*Present address: NEST, Istituto Nanoscienze-CNR and Scuola Normale Superiore, I-56127 Pisa, Italy.
†fabien.portier@cea.fr

[1] Y. Blanter and M. Büttiker, Phys. Rep. **336**, 1 (2000).
[2] G.-L. Ingold and Y. V. Nazarov, in *Single Charge Tunneling*, edited by H. Grabert and M. H. Devoret (Plenum, New York, London, 1992).
[3] A. N. Cleland, J. M. Schmidt, and J. Clarke, Phys. Rev. B **45**, 2950 (1992).
[4] P. Delsing, K. K. Likharev, L. S. Kuzmin, and T. Claeson, Phys. Rev. Lett. **63**, 1180 (1989).
[5] L. J. Geerligs, V. F. Anderegg, C. A. van der Jeugd, J. Romijn, and J. E. Mooij, Europhys. Lett. **10**, 79 (1989).
[6] A. V. Galaktionov, D. S. Golubev, and A. D. Zaikin, Phys. Rev. B **68**, 085317 (2003).
[7] M. Kindermann and Y. V. Nazarov, Phys. Rev. Lett. **91**, 136802 (2003).
[8] M. Kindermann, Y. V. Nazarov, and C. W. J. Beenakker, Phys. Rev. B **69**, 035336 (2004).
[9] I. Safi and H. Saleur, Phys. Rev. Lett. **93**, 126602 (2004).
[10] H. Lee and L. S. Levitov, Phys. Rev. B **53**, 7383 (1996).
[11] See Supplemental Material at http://link.aps.org/supplemental/10.1103/PhysRevLett.112.236803 for more information.
[12] G. B. Lesovik and R. Loosen, JETP Lett. **65**, 295 (1997). Here the distinction is made between emission noise $S_I(\nu) = 2\int_{-\infty}^{\infty}\langle I(t)I(0)\rangle e^{-i2\pi\nu t}dt$ and absorbtion noise $S_I(-\nu)$. While observation of the later requires excitation of the sample by external sources, for a zero temperature external circuit, only $S_I(\nu)$ is observed. For an earlier high-frequency shot noise derivation not making the distinction between $S_I(\nu)$ and $S_I(-\nu)$; see V. A. Khlus, Zh. Eksp. Teor. Fiz. **93**, 2179 (1987) [Sov. Phys. JETP **66**, 1243 (1987), http://www.jetp.ac.ru/cgi-bin/e/index/r/93/6/p2179?a=list]; G. B. Lesovik, Pis'ma Zh. Eksp. Teor. Fiz. **49**, 513 (1989), http://www.jetpletters.ac.ru/ps/229/article_3821.shtml [JETP Lett. **49**, 592 (1989), http://www.jetpletters.ac.ru/ps/1120/article_16970.shtml].
[13] S. Kafanov and P. Delsing, Phys. Rev. B **80**, 155320 (2009).
[14] S. Gustavsson, R. Leturcq, B. Simovič, R. Schleser, P. Studerus, T. Ihn, K. Ensslin, D. C. Driscoll and A. C. Gossard, Phys. Rev. B **74**, 195305 (2006).
[15] M. A. Castellanos-Beltran, K. D. Irwin, G. C. Hilton, L. R. Vale, and K. W. Lehnert, Nat. Phys. **4**, 929 (2008).
[16] E. Chow, P. Delsing, and D. B. Haviland, Phys. Rev. Lett. **81**, 204 (1998).
[17] P. Joyez, D. Esteve, and M. H. Devoret, Phys. Rev. Lett. **80**, 1956 (1998).
[18] B. Huard, H. Pothier, D. Esteve and K. E. Nagaev, Phys. Rev. B **76**, 165426 (2007).
[19] M. Hofheinz, F. Portier, Q. Baudouin, P. Joyez, D. Vion, P. Bertet, P. Roche, and D. Esteve, Phys. Rev. Lett. **106**, 217005 (2011).
[20] T. Holst, D. Esteve, C. Urbina, and M. H. Devoret, Phys. Rev. Lett. **73**, 3455 (1994).
[21] R. J. Schoelkopf, P. J. Burke, A. A. Kozhevnikov, D. E. Prober, and M. J. Rooks, Phys. Rev. Lett. **78**, 3370 (1997).
[22] E. Onac, F. Balestro, L. H. W. van Beveren, U. Hartmann, Y. V. Nazarov, and L. P. Kouwenhoven, Phys. Rev. Lett. **96**, 176601 (2006).
[23] E. Zakka-Bajjani, J. Ségala, F. Portier, P. Roche, D. C. Glattli, A. Cavanna, and Y. Jin, Phys. Rev. Lett. **99**, 236803 (2007).
[24] S. Gustavsson, M. Studer, R. Leturcq, T. Ihn, K. Ensslin, D. C. Driscoll, and A. C. Gossard, Phys. Rev. Lett. **99**, 206804 (2007).
[25] U. Gavish, Y. Levinson, and Y. Imry, Phys. Rev. B **62**, R10637 (2000).
[26] R. Aguado and L. P. Kouwenhoven, Phys. Rev. Lett. **84**, 1986 (2000).
[27] L. Spietz, K. W. Lehnert, I. Siddiqi and R. J. Schoelkopf, Science **300**, 1929 (2003).
[28] D. S. Golubev and A. D. Zaikin, Phys. Rev. Lett. **86**, 4887 (2001).
[29] A. Levy Yeyati, A. Martin-Rodero, D. Esteve, and C. Urbina, Phys. Rev. Lett., **87**, 046802 (2001).
[30] R. Cron *et al.*, in *Electronic Correlations: From Meso to Nano-Physics*, edited by T. Martin, G. Montambaux, and J. T. T. Vân (EDPSciences, Les Ulis, 2001).
[31] C. Altimiras, U. Gennser, A. Cavanna, D. Mailly, and F. Pierre, Phys. Rev. Lett. **99**, 256805 (2007).
[32] J. R. Souquet, I. Safi and P. Simon, Phys. Rev. B **88**, 205419 (2013).
[33] F. D. Parmentier, A. Anthore, S. Jezouin, H. le Sueur, U. Gennser, A. Cavanna, D. Mailly, and F. Pierre, Nat. Phys. **7**, 935 (2011).
[34] S. Jezouin, M. Albert, F. D. Parmentier, A. Anthore, U. Gennser, A. Cavanna, I. Safi, and F. Pierre, Nat. Commun. **4**, 1802 (2013).
[35] H. T. Mebrahtu, I. V. Borzenets, D. E. Liu, H. Zheng, Y. V. Bomze, A. I. Smirnov, H. U. Baranger, and G. Finkelstein, Nature (London) **488**, 61 (2012).